

# A Numerical Estimate of the Small- $k_T$ Region in the BFKL Pomeron

J. Bartels<sup>1</sup>, H. Lotter<sup>1</sup>, and M. Vogt<sup>2</sup>

<sup>1</sup> *II. Institut für Theoretische Physik, Universität Hamburg \**

<sup>2</sup> *Deutsches Elektronen Synchrotron DESY, Hamburg*  
hep-ph/9511399

## Abstract

A computer study is performed to estimate the influence of the small- $k_T$  region in the BFKL evolution equation. We consider the small-x region of the deep inelastic structure function  $F_2$  and show that the magnitude of the small- $k_T$  region depends on  $Q^2$  and  $x_B$ . We suggest that the width of the  $\log k_T^2$ -distribution in the final state may serve as an additional footprint of BFKL-dynamics. For diffractive dissociation it is shown that the contribution of the infrared region is large - even for large  $Q^2$ . This contribution becomes smaller only if restrictions on the final state are imposed.

1.) Deep inelastic electron proton scattering at HERA has put strong emphasis on small-x physics. Both the observed rise of  $F_2$  at small x and the discovery of the large rapidity gap events have raised the question of how to connect these observations with the perturbative Balitskii, Fadin, Kuraev, Lipatov (BFKL) Pomeron [1] and the (nonperturbative) soft Pomeron [2] seen in hadron hadron scattering at high energies.

In the context of the deep inelastic structure functions the BFKL Pomeron suggests the possibility of calculating, for a not too small momentum scale  $Q_0^2$ , the x-dependence of the input gluon distribution which then enters the DGLAP [3] evolution equations. The main result is the power-like increase  $xg(x, Q^2) \sim (1/x)^{\omega_{\text{BFKL}}}$  with  $\omega_{\text{BFKL}} = \frac{N_c \alpha_s}{\pi} 4 \log 2 \approx 0.5$ . Such an increase is consistent with the data, but the preferred power is slightly smaller: for the gluon distribution  $xg(x, Q^2)$  the observed power lies in the interval  $\omega_{\text{exp}} = 0.3 \dots 0.4$  [4], and for  $F_2$  one finds a power in the range  $0.2 \dots 0.4$ . A recent analysis [4] leads to the conclusion that the experimental results are compatible with the BFKL interpretation, but the evidence is not yet compelling.

Unfortunately, numerical predictions based upon the BFKL approximation have several principal uncertainties. Most important is the observation that, as a result of the diffusion of  $\log k_T^2$ , the internal transverse momenta of the BFKL ladders may become arbitrarily small, and the contribution from this region of phase space cannot be extracted reliably within the leading logarithmic approximation. One expects that in this region higher order corrections will be very important, and

---

\*Supported by Bundesministerium für Forschung und Technologie, Bonn, Germany under Contract 05 6HH93P(5) and EEC Program "Human Capital and Mobility" through Network "Physics at High Energy Colliders" under Contract CHRX-CT93-0357 (DG12 COMA)

eventually nonperturbative effects will come into play. A convenient way of taking into account higher order perturbative QCD effects is the replacement of the fixed coupling constant by the running  $\alpha_s$ . This *ad hoc* procedure, however, is somewhat arbitrary: the BFKL ladders represent the leading logarithmic approximation, and the QCD coupling constant is frozen at the scale set by the external particles (e.g. the virtuality of the scattering gluons). The introduction of the running coupling is equivalent to taking into account a certain subset of nonleading corrections, but is clearly incomplete and misses out other important corrections. Moreover, the presence of the Landau pole in  $\alpha_s(k_T^2)$  requires an infrared cutoff which again represents a model dependent choice. These uncertainties, clearly, will be most severe if, in a given application, the BFKL Pomeron receives a large contribution from the infrared region. Therefore, a first estimate of the reliability of a BFKL prediction is a numerical study of the magnitude of the infrared region in the BFKL evolution (with fixed coupling  $\alpha_s$ ). If it turns out that the contribution of the infrared region is small, there seems to be no strong need of introducing the running coupling, and the BFKL calculation can be expected to be rather safe.

From this point of view the safest place to test the BFKL prediction at HERA is the inclusive measurement of forward jets [5, 6]: here the BFKL Pomeron has large momentum scales at both of its ends (the large photon mass and the transverse momentum of the observed jet). Consequently, the diffusion into the infrared region is expected to be small. This has been confirmed in a numerical analysis of the BFKL evolution [7]. The deep inelastic structure function  $F_2$ , on the other hand, is not a particularly suitable place to test the BFKL Pomeron. The large momentum scale of the photon mass provides a justification for applying perturbation theory, but the proton at the other end of the BFKL ladder pulls the momentum scale down to small momentum, and during the BFKL evolution the infrared region may contribute a quite significant amount. In order to obtain a more precise estimate of the magnitude of this “dangerous“ region again a computer analysis is needed, quite analogous to [7]. Another place at HERA where the BFKL Pomeron might play an important role is the diffractive dissociation of the photon. Apart from analytic considerations [8, 9] so far no estimate of the contribution of small  $k_T^2$  to the BFKL evolution has been performed.

**2.)** In this letter we present the results of a numerical calculation of the BFKL Pomeron for  $F_2$ , following the strategy of [7]: writing the BFKL equation (with fixed  $\alpha_s$ ) as an evolution equation in  $y = \log 1/x$ , we start the evolution at some initial value  $x_0$ , evolve in  $y$  and compute, as a function of  $y$ , the distribution in the logarithm of the transverse momentum,  $\log k_T^2$ . In our choice of the physical parameters we follow [10]: we take  $x_0 = 10^{-2}$  and evolve down to the HERA value of  $x = 10^{-4}$ . The initial  $k_T$ -distribution  $f_0$  is calculated from a recent GRV-parameterization [11] of the gluon density function of the proton. We model the nonperturbative region below  $Q_0^2 = 1.5 \text{ GeV}^2$  by using the ansatz [10]

$$f_0(x, k_T^2) = C \frac{k_T^2}{k_T^2 + Q_0^2}. \quad (1)$$

The constant  $C$  has been chosen in such a way that continuity of  $f_0$  at  $Q_0^2$  is guaranteed. At the end of the evolution we convolute the gluon distribution with the quark loop [12], where the quarks are taken to be massless. A first analysis in this direction but with the ansatz (1) taken for the whole  $k_T^2$ -range was presented in [13].

Results are shown in Fig.1. The straight line in the center denotes, as a function of  $y$ , the mean

value, whereas the curved lines to the left and the right mark the mean square deviation from the mean value. We have considered two different values for  $Q^2$ :  $10 \text{ GeV}^2$  (Fig. 1a) and  $100 \text{ GeV}^2$  (Fig. 1b). One observes that a large value of  $Q^2$  “drags“ the distribution towards larger values, i.e. away from the dangerous infrared region. Nevertheless, at the upper end the mean value stays somewhat below the photon mass  $Q^2$ . Increasing, on the other hand, the available rapidity interval, one makes the integration region broader and, hence, increases the influence of the infrared domain. In summary, one feels that the application of the BFKL Pomeron for  $F_2$ , in particular for the lower  $Q^2$  value, is somewhat uncertain. Most likely, nonleading corrections to the BFKL Pomeron cannot be neglected in this region; the calculation of these corrections therefore appears to be quite urgent.

In order to provide further evidence for BFKL dynamics and, in particular, to discriminate between BFKL and DGLAP dynamics, it is useful to look into the distribution of transverse energy in the final state. Some time ago it has been argued [14] that a measurement of the mean transverse energy  $\langle E_T \rangle$  of produced jets could be used to discriminate between a “BFKL“ and a “DGLAP“ final state. Namely, because of the absence of the strong  $k_T$ -ordering in the BFKL case, one expects a larger mean value  $\langle E_T \rangle$  than in the DGLAP-case. Moreover, the dependence upon  $x$  is quite different in both cases. For the BFKL case the general trend can be read off from the distributions shown in Fig. 1a - 1b. For simplicity we study the  $\langle E_T \rangle$  of the t-channel gluons which is not exactly the same as that of the produced jet. One should however expect that, qualitatively, both variables show the same behavior. We focus on the center in pseudorapidity in the hadronic center of mass system and study the mean value in  $\log k_T^2$  and the mean spread to the right and the left. By lowering  $x_B$  (i.e. increasing the length in rapidity) one observes an increase of the width; for the mean value there is no visible motion. In order to study these qualitative expectations in more detail, we show, in Fig. 2a, the distribution in  $\log k_T^2$  in the center of the rapidity interval between the photon and the proton, varying the overall length in rapidity. One sees that the maxima do not move when rapidity increases whereas the width clearly increases with growing rapidity. Simple analytic considerations in fact show that the maximum does not move. For the width the random walk mechanism in the BFKL Pomeron leads to the prediction:

$$\begin{aligned} \Delta(\log k_T^2) &= \sqrt{\frac{N_c \alpha_s}{\pi} 28\zeta(3) y} , \\ y &= \frac{(\alpha_1 + \frac{1}{2} \log \frac{1}{x_B} \frac{k_{J,T}^2}{Q^2})(\alpha_2 - \frac{1}{2} \log \frac{x_B}{x_0^2} \frac{k_{J,T}^2}{Q^2})}{\alpha_1 + \alpha_2 + \log \frac{x_0}{x_B}} . \end{aligned} \quad (2)$$

Here  $\alpha_1$  and  $\alpha_2$  are determined by the width of the boundary distributions at  $x_B$  and  $x_0$ . For  $k_{J,T}^2$  we choose a value of  $2 \text{ GeV}^2$  which is an estimate based on the mean  $k_T^2$  displayed in Figs. 1a - 1b. Fig. 2b shows the growth of the width with increasing rapidity. For comparison we display the analytic prediction (2) for  $Q^2 = 100 \text{ GeV}^2$ . For small  $x_B$  the analytic curve approaches the numerical one. We therefore conclude that the behavior of the width (in  $\log k_T^2$ ) may be a good signal for BFKL dynamics in the final state. In [10, 15] the variable  $E_T$  has been used to study “footprints“ of the BFKL Pomeron. From the  $\log k_T^2$  - distributions presented in Fig. 2a we have calculated the distributions in  $E_T = k_T = \exp \frac{1}{2} \log k_T^2$ . The growth of  $\langle E_T \rangle$  shown in Fig. 2c, indeed, presents a characteristic BFKL signal. The analytic prediction for this observable is

$$\langle E_T \rangle = \exp \left[ \frac{N_c \alpha_s}{\pi} \frac{7}{2} \zeta(3) y + \frac{1}{2} \xi \right] , \quad (3)$$

$$\xi = \frac{\langle \log k_{1,T}^2 \rangle (\alpha_2 - \frac{1}{2} \log \frac{x_B}{x_0} \frac{k_{J,T}^2}{Q^2}) + \langle \log k_{2,T}^2 \rangle (\alpha_1 + \frac{1}{2} \log \frac{1}{x_B} \frac{k_{J,T}^2}{Q^2})}{\alpha_1 + \alpha_2 + \log \frac{x_0}{x_B}}.$$

It depends on the mean  $\log k_{i,T}^2$  ( $i = 1, 2$ ) of the two boundary contributions. The difference seen in the  $x_B$ -dependence of  $\langle \log k_T^2 \rangle$  (Fig. 2a) and  $\langle E_T \rangle$  (Fig. 2c) indicates that the latter quantity already feels the increase of the width. From the point of view of BFKL predictions, however, the variable  $\log k_T^2$  and its width seem to be more natural.

As far as comparison with experiment is concerned, for the mean value  $\langle E_T \rangle$  of produced jets, there is evidence [15] that the data are, in fact, closer to the BFKL-type distribution than to DGLAP; however, in the comparison with the data, the “theoretical predictions“ are presented by two different Monte Carlos which are neither pure BFKL nor DGLAP. It is, on the other hand, quite clear that the hadronization effects will lead to changes of the analytical predictions. For the width an analysis along this line has not yet been done.

**3.)** Another place where the BFKL Pomeron may potentially become important is the measurement of the diffractive dissociation of the photon. *A priori*, it is not clear whether the Pomeron which is responsible for the rapidity gap is the same as the one seen in hadron hadron scattering or whether it is more close to the hard Pomeron seen in  $F_2$ . Following a straightforward partonic picture of this process, one is lead to the conclusion that the integrated cross section (at fixed mass  $M$  of the diffractive system) should be a superposition of both types of the Pomeron, the hard and the soft one. The process is most conveniently discussed in the proton rest frame: at small  $x$ , the photon splits into a  $q\bar{q}$  pair, and the lifetime of this fluctuation is of the order  $1/2M_p x$ . In the simplest case the final state of the photon consists just of this quark-antiquark pair which scatters elastically off the proton. The dynamics of the elastic scattering now depends crucially upon the kinematic configuration of the  $q\bar{q}$ -pair. If the transverse momenta are small and the mass  $M$  of the system is of the order of  $\sqrt{Q^2}$ , the longitudinal momenta should be rather asymmetric, i.e. one of the quarks carries almost all the longitudinal momentum of the photon, whereas the momentum fraction of the other one is small. In the  $\gamma^* - IP$  rest system the produced quark and antiquark are almost collinear with the proton direction (“aligned jet model“ [16]). Since the elastic scattering of a quark with small virtuality is expected to proceed via the soft Pomeron, this final state configuration will be dominated by the soft Pomeron and its characteristic energy dependence. In addition to this configuration, however, there is also the final state with larger transverse momenta. In this case one expects the elastic scattering of the  $q\bar{q}$ -system to proceed via the exchange of the hard Pomeron, e.g. a perturbative BFKL ladder. A signal of this would be a steeper energy dependence of the cross section. Combining these two possibilities, one expects to see both the hard and the soft Pomeron, each of them being associated with specific final state configurations. As to the question which of them will be dominant, there seems to be, at least within this picture, a slight preference for the soft configuration: a quark with a large transverse size has a larger cross section than a small-size object. On the other hand, the appearance of the hard Pomeron which at large energies grows stronger than the soft one enhances the cross section of the hard diffractive final state. Clearly a careful study of QCD models based upon the BFKL Pomeron will be a valuable way of studying this competition between the hard and the soft component.

In order to discuss the experimental situation we need a few formulae. Arguments based upon

triple Regge analysis [18, 19, 20] suggest to write the cross section in the following form:

$$\frac{d^4\sigma}{dx dQ^2 dx_{\mathcal{P}} dt} = \frac{4\pi\alpha^2}{xQ^2} \left(1 - y + \frac{y^2}{2}\right) F_2^{\mathcal{P}}(\beta, Q^2, t) \left(\frac{1}{x_{\mathcal{P}}}\right)^{2\alpha(t)-1} \frac{\beta_{\mathcal{P}}^2(t)}{16\pi}, \quad (4)$$

where  $x_B = \frac{Q^2+M^2-t}{Q^2+W^2}$ ,  $\beta = x/x_{\mathcal{P}} = \frac{Q^2}{Q^2+M^2-t}$ , and we have neglected the longitudinal part of the Pomeron structure function. The soft Pomeron [2] requires the exponent of  $1/x_{\mathcal{P}}$  to have the value  $2\alpha(0) - 1 = 1.17$ , whereas the hard Pomeron belongs to  $2\alpha(0) - 1 > 1.4$  (if one uses the power 0.2 for the hard Pomeron at 20 GeV<sup>2</sup>), or even  $2\alpha(0) - 1 \approx 2$  for the BFKL Pomeron. Experimental values for the exponent of  $\frac{1}{x_{\mathcal{P}}}$  are [20, 21, 22]:

H1	1.19	$\pm 0.06$	$\pm 0.07$
ZEUS	1.30	$\pm 0.08$	$\begin{smallmatrix} +0.08 \\ -0.14 \end{smallmatrix}$
ZEUS	1.47	$\pm 0.03$	$\begin{smallmatrix} +0.14 \\ -0.10 \end{smallmatrix}$

The third value is based upon a new method of defining the nondiffractive background. Obviously, the first value is close to the soft Pomeron, i.e. in most of the events the final state is such that the soft Pomeron dominates. The third value, on the other hand, seems to favor the hard Pomeron. [20, 21] also present evidence for the factorization in (4): within the errors, the power of  $1/x_{\mathcal{P}}$  does not vary with  $Q^2$  or  $\beta$ .

Perturbative QCD calculations of diffractive dissociation are contained in [23, 24, 25]; a consistent BFKL-type calculation has been presented in [8]. The latter one, being based upon the BFKL approximation, also includes small transverse momenta for the produced diffractive system consisting of  $q\bar{q} + gluons$ . Therefore it allows, in particular, to answer the question which transverse momenta the BFKL Pomeron predicts for the final state. Analytic estimates based upon the results of [8] show that the preferred  $k_T$  value at the upper end of the BFKL Pomeron in diffractive DIS dissociation is rather low. In other words, in this process the BFKL Pomeron seems to get its main contribution from the region of small  $k_T$  where higher order corrections are expected to be essential. Their main effect will be the lowering of the exponent  $\omega_{\text{BFKL}}$ . Since we do not know yet the corrections to BFKL, we are presently unable to make a quantitative prediction.

4.) Starting from the cross section formula for the diffractive production of  $q\bar{q}$  pairs (at  $t = 0$ ) we have performed a numerical analysis of the BFKL Pomeron, very much in the same spirit as we did for  $F_2$ . The coupling to the proton is done in the same way as in  $F_2$  (see above). In Figs. 3a – 3d we show, as a function of rapidity, the distribution of the transverse momentum inside the BFKL ladder. We begin with the integrated (over invariant mass  $M$  and transverse momenta of the outgoing quarks) cross section in Figs. 3a and 3b. Most striking is the trend of the mean value to be small at the upper end (i.e. the coupling to the  $q\bar{q}$ ): increasing the photon mass  $Q^2$  seems to pull the upper value to the right, but it does not exceed the hadronic scale at the lower end (i.e. the coupling to the proton). This fully confirms the findings of [9], and we are lead to the conclusion that the BFKL Pomeron in diffractive dissociation gets its main contributions from a region where the corrections should be large. Based upon the observed behavior of  $F_2$  we expect that these corrections will mainly lead to a lowering of the increase in  $1/x_{\mathcal{P}}$ , i.e. to the change from the hard Pomeron to the soft one. Next we undo the integration over the final state: at fixed values for  $Q^2$  (20 GeV<sup>2</sup>) we plot the cross section (integrated over the invariant mass  $M$ ) for different values of the transverse momenta of the outgoing quarks: Figs. 3c and 3d ( $p_T^2 = 1 \text{ GeV}^2$  and  $5 \text{ GeV}^2$  resp.)

show the clear trend that a large  $p_T$  pulls the scale at the upper end of the Pomeron to the right and thus makes the Pomeron harder. This is consistent with the calculations [26, 27] of the cross section for the production of heavy vector mesons from longitudinal photons: in the coupling of the pomeron to the  $q\bar{q}$  - state large  $p_T^2$  dominate and one expects the hard pomeron to become important. Recent HERA data [28] seem to support this prediction.

This result has implications for the applicability of perturbative models to the process of diffractive dissociation. In earlier models [23, 24, 25] it was assumed that the final states had to be hard. The model in [8] which has been used in this letter, has the advantage that it is well-defined also in the small- $k_T$  region. The analysis, however, has led to the conclusion that the hard final states are only a minor part of the cross section, and for a reliable calculation higher order corrections are unavoidable. A first attempt to model higher order effects has been made recently [29]: by replacing the fixed power of the BFKL Pomeron by a variable one (being a function of the scale of the  $q\bar{q}$  pair), an effective transition from the hard to the soft Pomeron has been included. Further work in this direction appears to be very promising.

As an experimental consequence of our study we expect that events with hard  $q\bar{q}$  - final states will get a larger contribution from the hard pomeron. As a first guideline one may trigger on events with large  $p_T^2$  (in the  $\gamma^* - p$  center of mass system). A more accurate estimate of the hardness of the pomeron may be  $p_T^2(Q^2 + M^2)/M^2$  which, in the aligned jet model, would correspond to the virtuality of one of the two quarks in which the photon dissociates.

**5.)** More generally, the behavior of the BFKL Pomeron in diffractive dissociation may shed some light on the way in which the unitarization of the BFKL Pomeron works. It is generally believed that among the next-to-leading order corrections to the BFKL Pomeron those with a larger number of t-channel gluon lines ( $n > 2$ ) will play the most important role in unitarizing the BFKL approximation. The cross section for diffractive dissociation (as discussed in, e.g., [8]) constitutes a measurable part of these corrections. Consequently, a measurement of the cross section and the comparison with the calculation can be used to estimate the magnitude of unitarity corrections, and a detailed study of models can teach us how unitarization will work. As to the discussion presented in this letter, the main conclusion in this direction seems to be that unitarization of the BFKL Pomeron begins mainly in the small- $k_T$  region.

## References

- [1] E.A.Kuraev, L.N.Lipatov, V.S.Fadin, *Sov.Phys.JETP* **45** (1977) 199;  
Ia.Ia.Balitskii and L.N.Lipatov, *Sov.J.Nucl.Phys.* **28** (1978) 822.
- [2] A.Donnachie and P.V.Landshoff, *Phys.Lett.* **B 296** (1992) 227.
- [3] V.N.Gribov and L.N.Lipatov, *Sov. J.Nucl.Phys.* **15** (1972) 438 and 675;  
G.Altarelli and G.Parisi, *Nucl.Phys.* **B 126** (1977) 298;  
Yu.L.Dokshitzer, *Sov.Phys.JETP* **46** (1977) 641.
- [4] H1 Collaboration, *Phys. Lett.* **B 354** (1995) 494.
- [5] A.H.Mueller, *Nucl.Phys.B* (Proc.Suppl.) **18 C** (1991) 125;  
J. Bartels, A.DeRoeck, M.Loewe, *Z.Phys.* **C 54** (1992) 635;  
J.Bartels, M.Besancon, A.De Roeck, J.Kurzhofer, in: *Proceedings of the HERA Workshop 1992* (eds.W.Buchmüller and G.Ingelman), p.203;  
J.Kwieciński, A.D.Martin, P.J.Sutton, *Phys.Lett.* **B 287** (1992) 254; *Phys.Rev.* **D 46** (1992) 921;  
W.-K.Tang, *Phys.Lett.* **B 278** (1991) 363.
- [6] J.Bartels, V.DelDuca, A.DeRoeck, D.Graudenz, M.Wüsthoff, DESY preprint in preparation.
- [7] J.Bartels and H.Lotter, *Phys.Lett.* **B 309** (1993) 400.
- [8] J.Bartels and M.Wüsthoff, *Zeitschr.Phys.* **C 66** (1995) 157.
- [9] J.Bartels, H.Lotter, M.Wüsthoff, *Zeitschr.Phys.* **C 68** (1995) 121.
- [10] A.J.Askew, J.Kwieciński, A.D.Martin, P.J.Sutton, *Phys.Rev.* **D 49** (1994) 4402.
- [11] M.Glück, E.Reya, A.Vogt, *Z.Phys.***C 53** (1992) 127.
- [12] E.M.Levin and M.G.Ryskin, *Sov. Journ. Nucl. Phys.* **53** (1991) 653;  
W.K.Tang, *Phys. Lett.* **B 284** (1992) 123;  
J. Bartels, A.DeRoeck, M.Loewe, *Z.Phys.* **C 54** (1992) 635;  
J.Kwieciński, A.D.Martin, P.J.Sutton, *Phys.Lett.* **B 287** (1992) 254; *Phys. Rev.* **D 46** (1992) 921.
- [13] J.R.Forshaw, P.N.Harriman, P.J.Sutton, *Nucl. Phys.* **B 416** (1994) 739.
- [14] J.Kwieciński, A.D.Martin, P.J.Sutton, K.Golec-Biernat, *Phys.Rev.***D 50** (1994) 217;  
K.Golec-Biernat, J.Kwieciński, A.D.Martin, P.J.Sutton, *Phys.Lett.* **B 335** (1994) 220.
- [15] H1 Collaboration, DESY-95-108 and *Phys.Lett.* **B 356** (1995) 118.
- [16] V.N.Gribov, B.L.Ioffe, I.Ya.Pomeranchuk, *Yad.Fiz.* **2** (1965) 768;  
B.L.Ioffe, *Phys.Lett.* **30** (1968) 123;  
C.Llewellyn-Smith, *Phys.Rev.* **D 4** (1971) 2392;  
V.N.Gribov, *Sov.Phys.JETP* **30** (1969) 709 and *ITEP School on Elementary Particles* (1973) Vol.I, p.53;

- J.D.Bjorken in *Proceedings of the International Symposium on Electron and Photon Interactions at High Energies*, p.281 (Cornell 1971);  
L.Frankfurt and M.Strikman, *Phys.Rep.* **160** (1988) 235.
- [17] G.Ingelman and P.Schlein, *Phys.Lett.* **B 152** (1985) 256.
- [18] E.L.Berger, J.C.Collins, E.Soper, G.Sterman, *Nucl.Phys.* **B 286** (1987) 704.
- [19] G.Ingelman and K.Prytz, *Zeitschr.Phys.* **C 58** (1993) 285.
- [20] H1 Collaboration, *Phys.Lett.* **B 348** (1995) 681.
- [21] ZEUS Collaboration, DESY-95-093.
- [22] ZEUS Collaboration, Contribution submitted to the 17th International Symposium on Lepton - Photon Interactions, Beijing, China, August 1995.
- [23] M.G.Ryskin, *Sov.J.Nucl.Phys.* **52** (1990) 529.
- [24] N.N.Nikolaev and B.G.Zakharov, *Zeitschr.Phys.* **C 53** (1992) 331.
- [25] E.Levin and M.Wüsthoff, *Phys.Rev.* **D 50** (1994) 4306.
- [26] M.G.Ryskin, *Zeitschr.Phys.* **C 57** (1993) 89.
- [27] S.J.Brodsky, L.Frankfurt, J.F.Gunion, A.H.Mueller, M.Strikman, *Phys. Rev.* **D 50** (1994) 3134.
- [28] H1 Collaboration, *Phys. Lett.* **B 338** (1994) 507;  
ZEUS Collaboration, *Phys. Lett.* **B 350** (1995) 120; *Phys. Lett.* **B 356** (1995) 601.
- [29] M.Wüsthoff, PhD Thesis, Hamburg 1995 and DESY-95-166.



## Figure captions

Fig. 1a : Mean value and root mean square deviation of the distribution of  $\log k_T^2$  inside the BFKL–evolution for  $F_2$ . The values of  $x_B$  and  $Q^2$  are  $10^{-4}$  and  $10 \text{ GeV}^2$ . The variable  $x$  gives the position on the BFKL ladder at which these quantities are measured.

Fig. 1b : The same as in Fig. 1a but with  $x_B = 10^{-4}$  and  $Q^2 = 100 \text{ GeV}^2$ .

Fig. 2a : Normalized distribution of  $\log k_T^2$  inside the BFKL–evolution for  $F_2$  with  $Q^2 = 100 \text{ GeV}^2$  and three different values of  $x_B$ , measured at a rapidity value of  $\frac{1}{2} \log \frac{10^{-2}}{x_B}$ . Values of  $x_B$  are  $5 \cdot 10^{-3}$  (the curve with the highest peak),  $10^{-3}$  and  $5 \cdot 10^{-4}$  (the curve with the lowest peak).

Fig. 2b : Dependence of the the root mean square deviation of the distributions of Fig. 2a on  $x_B$  for  $Q^2 = 100, 30$  and  $15 \text{ GeV}^2$  (from top to bottom). The dotted line shows the analytic prediction eq. (2) for  $Q^2 = 100 \text{ GeV}^2$ .

Fig. 2c : Dependence of the mean transverse energy  $E_T = \exp \frac{1}{2} \log k_T^2$  of the distributions of Fig. 2a on  $x_B$  shown for values of  $Q^2 = 100, 30$  and  $15 \text{ GeV}^2$  (from top to bottom).

Fig. 3a : Mean value and root mean square deviation of the  $\log k_T^2$  distribution inside the BFKL–evolution in totally inclusive diffractive dissociation. Values of  $x_B$  and  $Q^2$  are  $10^{-4}$  and  $10 \text{ GeV}^2$ .

Fig. 3b : The same as in Fig. 3a but with  $x_B = 10^{-4}$  and  $Q^2 = 100 \text{ GeV}^2$ .

Fig. 3c : Mean value and root mean square deviation of the  $\log k_T^2$  distribution inside the BFKL–evolution in the M – integrated diffractive dissociation with high  $p_T$ -quarks in the final state. We have taken  $x_B = 10^{-4}$ ,  $Q^2 = 20 \text{ GeV}^2$  and  $p_T^2 = 1 \text{ GeV}^2$ .

Fig. 3d : The same as Fig. 3c with  $x_B = 10^{-4}$ ,  $Q^2 = 20 \text{ GeV}^2$  and  $p_T^2 = 5 \text{ GeV}^2$ .

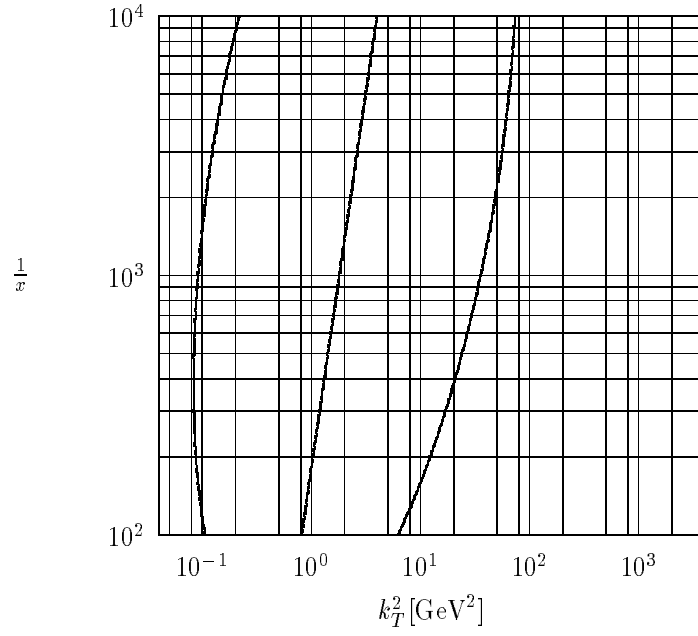


Figure 1a:

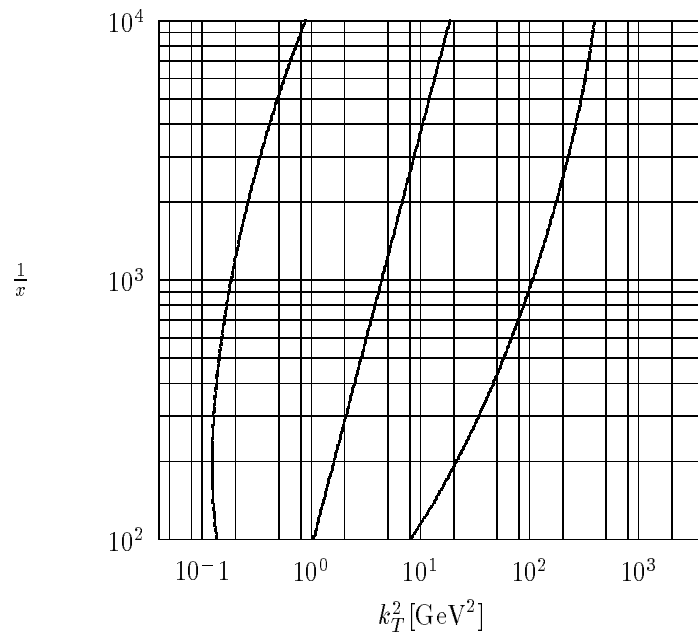


Figure 1b:

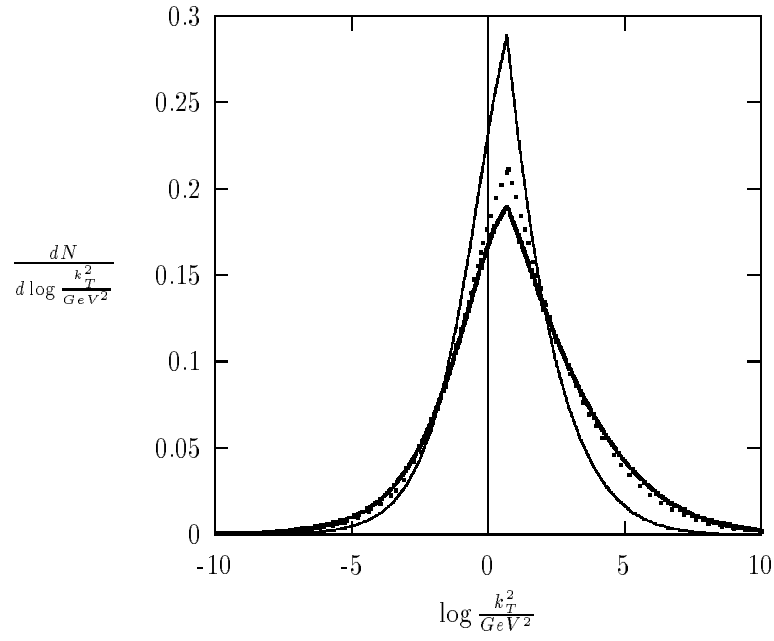


Figure 2a:

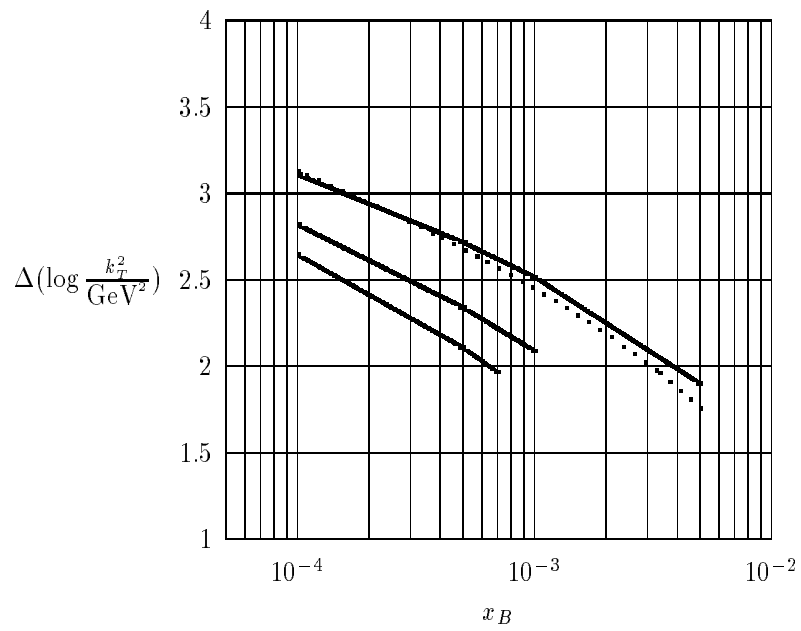


Figure 2b:

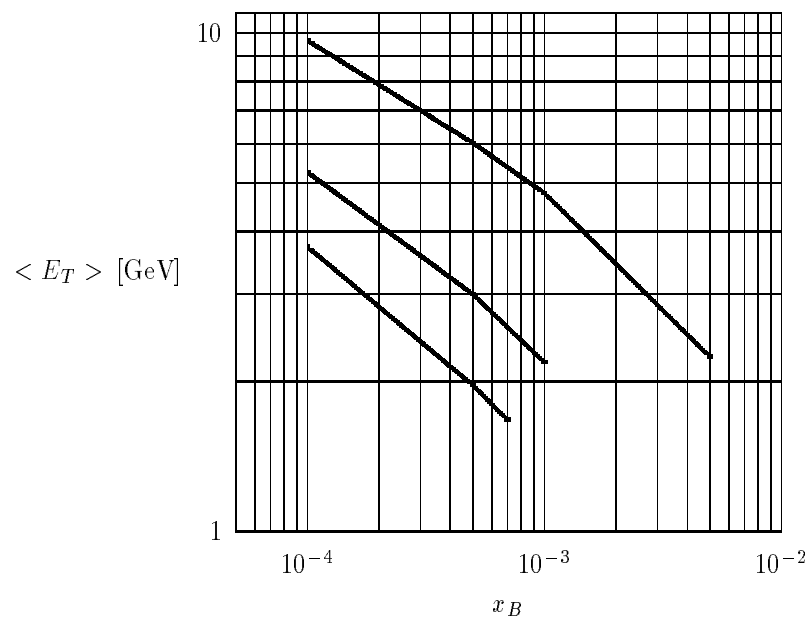


Figure 2c:

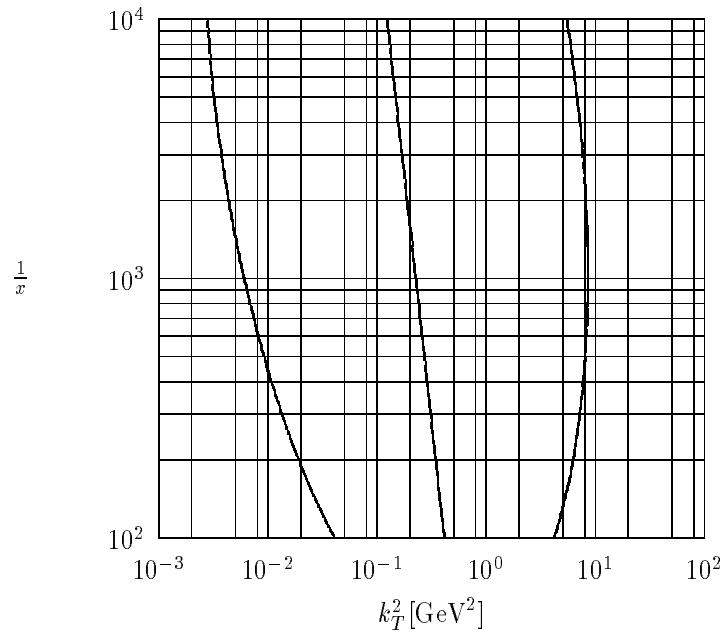


Figure 3a:

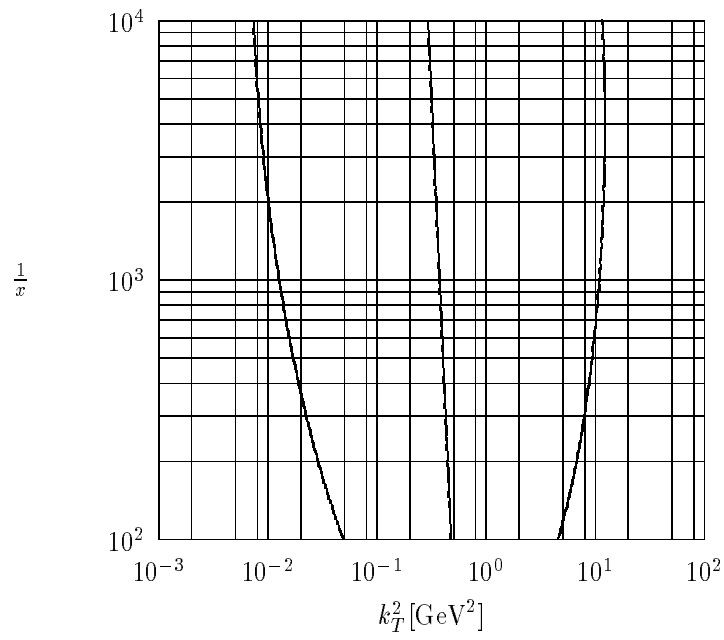


Figure 3b:

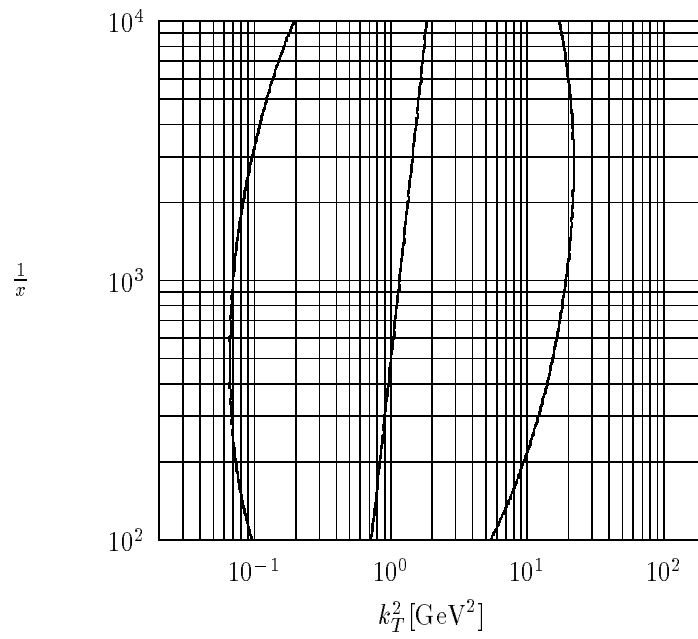


Figure 3c:

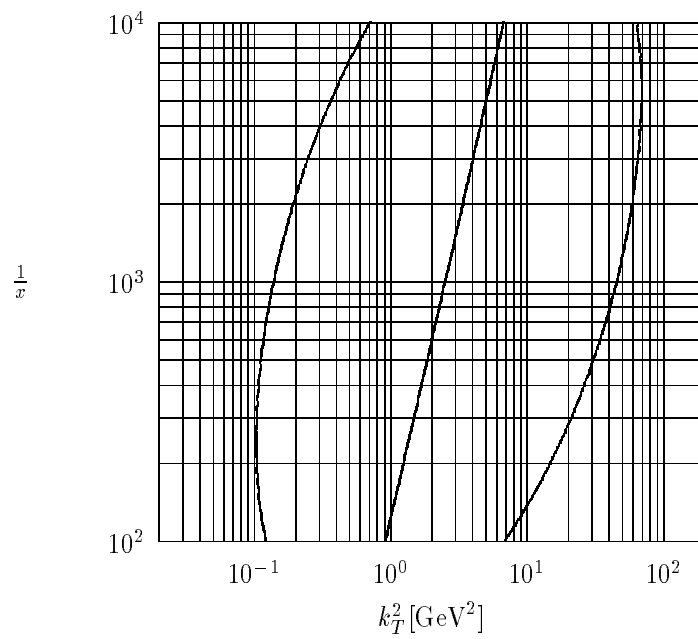


Figure 3d: